Optical Rotation Approach to Search for the Electric Dipole Moment of the Electron

Dmitry V. Chubukov [1,2,]* , Leonid V. Skripnikov [1,2], Vasily N. Kutuzov [1],
Sergey D. Chekhovskoi [1] and Leonti N. Labzowsky [1,2]

[1] Department of Physics, St. Petersburg State University, 7/9 Universitetskaya Naberezhnaya,
199034 St. Petersburg, Russia; leonidos239@gmail.com (L.V.S.); vas-kutuzow@yandex.ru (V.N.K.);
Reezeereezee@gmail.com (S.D.C.); l.labzovskii@spbu.ru (L.N.L.)

[2] Petersburg Nuclear Physics Institute named by B.P. Konstantinov of National Research Centre
"Kurchatov Institut", 188300 Gatchina, Russia

* Correspondence: dmitrybeat@gmail.com

Abstract: The $\mathcal{P},\mathcal{T}$-odd Faraday effect (i.e., rotation of the polarization plane of light propagating through a medium in presence of the external electric field due to $\mathcal{P}$, $\mathcal{T}$ symmetry violating interactions) is considered for several atomic species: Ra, Pb, Tl, Hg, Cs, and Xe. Corresponding theoretical simulation of $\mathcal{P},\mathcal{T}$-odd Faraday experiment, with already achieved intracavity absorption spectroscopy characteristics and parameters, is performed. The results show that the magnetic dipole transitions in the Tl and Pb atoms as well as the electric dipole transitions in the Ra, Hg and Cs atoms are favorable for the observation of the $\mathcal{P},\mathcal{T}$-odd Faraday optical rotation. The estimation of the rotation angle of the light polarization plane demonstrates that recently existing boundaries for the electron electric dipole moment can be improved by one-two orders of magnitude.

Keywords: optical rotation; electric dipole moment; $\mathcal{P},\mathcal{T}$-odd Faraday effect

1. Introduction

The study of the spatial parity ($\mathcal{P}$) and time reversal ($\mathcal{T}$) symmetry violation in atomic and molecular systems is of importance for physics of fundamental interactions. If the electron possesses a nonzero electric dipole moment (*e*EDM), it means simultaneous violation of $\mathcal{P}$ and $\mathcal{T}$ symmetries. Within the frames of the standard model (SM) of electroweak interactions, *e*EDM is predicted to be less than 10^{-38} *e* cm [1]. However, in numerous extensions of the SM the *e*EDM is predicted to have much larger values. As was shown in [2,3], the *e*EDM is strongly enhanced compared to the EDM of free electron in heavy atoms. Even stronger enhancement of the *e*EDM can arise in diatomic molecules containing heavy nucleus with open electron shells due to the existence of closely spaced energy levels of opposite parity. Note also that in atomic and molecular systems in an external electric field the effect of *e*EDM is always accompanied by another $\mathcal{P},\mathcal{T}$-odd effect—$\mathcal{P},\mathcal{T}$-odd interaction of electron and nucleus [4,5]. Various models for the $\mathcal{P},\mathcal{T}$-odd interactions in frames of the SM are discussed in [6,7]. In [5] it was also demonstrated that in an external electric fields both abovementioned $\mathcal{P},\mathcal{T}$-odd effects cannot be distinguished in any experiment with any particular atom or molecule. However, as was shown in [8] this can be done in the series of experiments with different species due to the different dependence of these effects on the nuclear charge Z. Please note that we do not consider here other sources of $\mathcal{P},\mathcal{T}$-violation effects including spin-dependent effects such as the interaction of the nuclear magnetic quadrupole moment with electrons [9] which will be considered elsewhere. The most restrictive bounds for the *e*EDM were established in the following experiments: with the Tl atom ($d_e < 1.6 \times 10^{-27}$ *e* cm) [10], YbF molecule ($d_e < 1.05 \times 10^{-27}$ *e* cm) [11],

ThO molecule ($d_e < 0.87 \times 10^{-28}$ *e* cm [12], $d_e < 1.1 \times 10^{-29}$ *e* cm [13]), and HfF$^+$ molecular ion ($d_e < 1.3 \times 10^{-28}$ *e* cm) [14] (*e* is the electron charge). However, to extract the *e*EDM values from the experimental data, the accurate calculations of the *e*EDM enhancement coefficients are required. These calculations were performed for Tl in [15–18], for YbF in [19–22], for ThO in [23–26] and for HfF$^+$ in [27–30].

The optical rotation experiments to study spatial parity nonconserving (PNC) effects (that is to say, the rotation of the light polarization plane in atomic or molecular vapors that do not possess natural optical activity) were originally proposed in [31] for hydrogen atom where parity nonconservation is very small. After a while in 1974 a new proposal with the Bi atom was discussed [32]. In addition, the first successful optical rotation experiment on the PNC effect observation in Bi was performed in 1978 [33]. What concerns the experiment on the search for the $\mathcal{P},\mathcal{T}$ symmetry violation effects, all of them up to now are advancing in two directions: the shift of the magnetic resonance in an external electric field [10] and the electron spin precession in an external electric field [11–14]. Since the recent experimental bound for the *e*EDM is still 9 orders of magnitude larger than the maximum theoretical prediction of the SM, other methods of the observation of such effects are of interest. The optical rotation in an external electric field can be referred to as the $\mathcal{P},\mathcal{T}$-odd analogue of the Faraday effect (the latter is the optical rotation in an external magnetic field). Unlike the ordinary Faraday effect, in an external electric field such optical rotation can arise only due to the violation of $\mathcal{P}$ and $\mathcal{T}$ symmetries. In [34] the possible existence of such an effect was discussed. Measurement of the *e*EDM using the Faraday rotation technique was suggested in [35]. Different theoretical and experimental studies were directed to observe it (see, e.g., short review [36]). Recently, in [37] the possibility of the $\mathcal{P},\mathcal{T}$-odd Faraday effect observation by means of the cavity-enhanced technique and intracavity absorption spectroscopy (ICAS) [38–40] was revisited. In [38] an experiment on the observation of the $\mathcal{P}$-odd optical rotation in the Xe, Hg, and I atoms was discussed. The techniques described in [38] can be applied for the observation of the $\mathcal{P},\mathcal{T}$-odd Faraday effect. In [18] the calculation of the enhancement factors and the evaluation of the $\mathcal{P},\mathcal{T}$-odd Faraday effect oriented to the techniques [38] for heavy atoms were carried out. In previous experiments [41] such heavy metal atoms were considered as the most suitable objects for the observation of the $\mathcal{P}$-odd optical rotation. Please note that the results for the $\mathcal{P},\mathcal{T}$-odd Faraday rotation signal given in [18] were overestimated for electric dipole (E1) transitions due to neglect of the natural line width. Calculations of the enhancement factors and the corresponding $\mathcal{P},\mathcal{T}$-odd Faraday effect for the Xe and Hg atoms considered in [38] as most suitable objects for the optical cavity experiments was performed in [42]. In the present paper we outline the theory of the $\mathcal{P},\mathcal{T}$-odd Faraday optical rotation and give estimates of the effect for different atomic species.

2. Theory of the $\mathcal{P},\mathcal{T}$-Odd Faraday Effect

When the light propagates through the optical active medium its polarization plane rotates. This rotation arises due to the difference in the refraction indices for left- (n^+) and right- (n^-) circularly polarized light:

$$\psi = \pi \frac{l}{\lambda} \text{Re} \left(n^+ - n^- \right) \tag{1}$$

where l is the optical path length, λ is the wave length of the light. In general, the refractive index for any resonant processes in any atomic (or molecular) system can be expressed via the scalar part of the dynamic polarizability tensor of this system $\alpha(\omega)$:

$$n(\omega) = \sqrt{1 + 4\pi\rho\alpha(\omega)} \approx 1 + 2\pi\rho\alpha(\omega). \tag{2}$$

Here ρ is the atomic vapor number density,

$$\alpha_i(\omega) = \frac{1}{3} \sum_f \frac{\left| A_{i \to f} \right|^2}{E_f - E_i - \omega - \frac{i}{2}\left(\Gamma_i + \Gamma_f + 2\Gamma_{\text{col}} \right)} \tag{3}$$

is the polarizability of the atomic state i, $A_{i \to f}$ is the transition amplitude between the initial i and final f atomic states. Γ_i, Γ_f are the corresponding natural line widths. Γ_{col} is the collisional broadening line width which is defined by the relation

$$\Gamma_{\text{col}} = \rho \sigma_{\text{col}} \sqrt{\frac{2k_B T}{M}}, \tag{4}$$

where σ_{col} is the collisional cross-section, k_B is the Boltzmann constant, T is the vapor temperature in Kelvin, M is the atomic mass. For electric dipole (E1) transitions Γ_{col} can be usually neglected compared to the natural line width of the excited atomic state. For magnetic dipole (M1) transitions the former line width can dominate at high number densities. Summation in Equation (3) should be extended over the entire atomic spectra. However, in the resonance case only one term corresponding to the particular level is retained.

Let us consider atomic vapor placed in a cavity with applied steady external electric field $\mathcal{E}$ along the direction of the light propagation. In what follows we ignore the hyperfine structure of atomic levels. In fact, it will be shown below that if the hyperfine structure is resolved, it does not change the order of magnitude for the estimate of the rotation angle. As a result of applying such an external field, the energy levels with a definite total electron angular momentum J begin to depend on the absolute value of the total electron angular momentum projection $|M_J|$. Taking into account the $\mathcal{P},\mathcal{T}$-odd effects such sublevel $|M_J|$ is split into two sublevels $M_J = \pm|M_J|$ with different energies (linear Stark effect). Then for the resonant case of the transition $iJ \to fJ'$ and different right- and left-circularly polarized light Equation (3) takes the following form:

$$\alpha_{iJ \to fJ'}^{\pm}(\omega) = \frac{1}{3} \frac{\left| A_{i,JM_J \to f,J'M_{J'}}^{\pm} \right|^2}{\omega_{i,JM_J;f,J'M_{J'}}^{\pm} - \omega - \frac{i}{2}\left(\Gamma_i + \Gamma_f + 2\Gamma_{\text{col}} \right)}, \tag{5}$$

where

$$\omega_{i,JM_J;f,J'M_{J'}}^{+} = E_{f,J'M_{J'}} - E_{i,JM_J}, \tag{6}$$

$$\omega_{i,JM_J;f,J'M_{J'}}^{-} = E_{f,J'\overline{M_{J'}}} - E_{i,J\overline{M_J}}. \tag{7}$$

In Equations (6) and (7) $\overline{M_J} = -M_J$, E_{i,JM_J} are the Stark split components of the electronic level iJ. $\mathcal{P},\mathcal{T}$-odd Faraday rotation arises only for such transitions which satisfy the condition

$$M_J - M_{J'} = \pm 1. \tag{8}$$
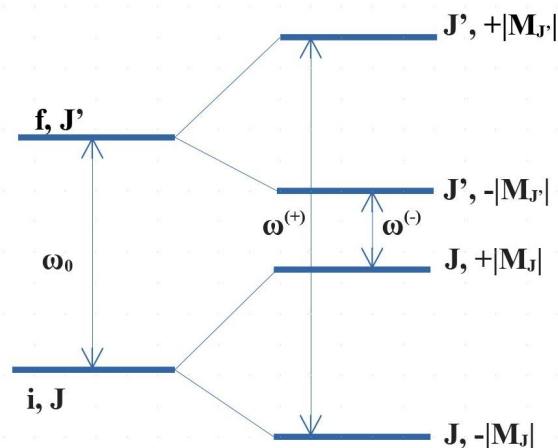
The scheme of such splitting is presented in Figure 1.

Figure 1. The scheme of the linear Stark splitting of the levels iJ and fJ'.

In what follows we only consider the linear Stark shift which is produced by the electron EDM. In case when the linear Stark shift is produced by the $\mathcal{P},\mathcal{T}$-odd pseudoscalar-scalar electron-nucleus interaction, in all formulas d_e should be replaced by the equivalent eEDM d_e^{eqv}, i.e., eEDM that leads to the same linear Stark shift in the same external electric field as the $\mathcal{P},\mathcal{T}$-odd electron-nucleus interaction [6]. A standard way of presenting linear Stark matrix element for the case of eEDM is as follows

$$\langle i, JM_J | S^{e\text{EDM}} | i, JM_J \rangle \equiv R_d d_e \mathcal{E} \tag{9}$$

where R_d is a dimensionless enhancement coefficient of the electron EDM in an atom:

$$R_d = \sum_{j>0} \frac{\langle i, JM_J | \sum_k -ez_k | \Psi_j \rangle \langle \Psi_j | V^{e\text{EDM}} / d_e | i, JM_J \rangle}{E_0 - E_j} + h.c. \tag{10}$$

The eEDM Hamiltonian $V^{e\text{EDM}}$ can be written in the following form [43,44]:

$$V^{e\text{EDM}} = d_e \frac{2i}{e\hbar} c\gamma^0 \gamma^5 \boldsymbol{p}^2, \tag{11}$$

where $\boldsymbol{p}$ is the electron momentum operator, γ^0 and γ^5 are the Dirac matrices, c is the speed of the light. Note also that instead of use of the direct sum-over-states method for the calculation of R_d (Equation (10)) one can use the finite difference method [45,46]. Such calculations of matrix elements (10) as well as transition amplitudes in the numerator of Equation (5) for atoms under consideration were performed in Refs. [18,42]. For this the relativistic coupled cluster method within the Dirac-Coulomb Hamiltonian has been used. Then the difference between ω^+ and ω^- can be expressed as

$$(\omega^+_{i,JM_J;f,J'M_{J'}} - \omega^-_{i,JM_J;f,J'M_{J'}}) = 2d_e\mathcal{E}\left(R_d[i, J|M_J|] + R_d[f, J'|M_{J'}|]\right). \tag{12}$$

Now introducing full effective line width $\Gamma = \Gamma_i + \Gamma_f + 2\Gamma_{\text{col}}$, omitting apparent indices and using Equations (2) and (5) one can rewrite the expression (1) in case of the $\mathcal{P},\mathcal{T}$-odd Faraday rotation as

$$\psi(\omega) = \frac{2\pi^2}{3} \frac{l}{\lambda} \rho |A|^2 \left\{ \frac{\omega^+ - \omega}{(\omega^+ - \omega)^2 + \frac{1}{4}\Gamma^2} - \frac{\omega^- - \omega}{(\omega^- - \omega)^2 + \frac{1}{4}\Gamma^2} \right\}. \tag{13}$$

Let us expand Equation (13) in terms of $d_e\mathcal{E}$ and retain only linear in electric field contribution. The next step is to take into account the chaotic motion of individual atoms in vapor and the Doppler

broadening, having applied the convolution of the Lorentz line profile with Maxwell distribution of atomic velocities. As a result of such transformation, the Voigt line profile appears. In what follows for the Voigt profile, we will use the parametrization adopted in [41]. The dispersive part of the Voigt profile which defines the refractive index $n(\omega)$ can be parametrized as

$$\text{Re } n(u) \sim \text{Im } \mathcal{F}(u, v) \equiv g(u, v). \tag{14}$$

The absorptive part is proportional to

$$\text{Im } n(u) \sim \text{Re } \mathcal{F}(u, v) \equiv f(u, v). \tag{15}$$

The function $\mathcal{F}(u, v)$ is defined as

$$\mathcal{F}(u, v) = \sqrt{\pi} e^{-(u+iv)^2} \left[1 - \text{Erf}(-i(u + iv)) \right] \tag{16}$$

where $\text{Erf}(z)$ is the error function, the variables u, v are defined as

$$u = \frac{\Delta \omega}{\Gamma_D} \tag{17}$$

and

$$v = \frac{\Gamma}{2\Gamma_D}, \tag{18}$$

respectively. Here $\Delta \omega$ is the detuning of the frequency and Γ_D is the Doppler width which is equal to

$$\Gamma_D = \omega_0 \sqrt{\frac{2k_B T}{Mc^2}}. \tag{19}$$

Now introducing the function $h(u, v) = \frac{dg(u,v)}{du}$ we find

$$\psi(u) = \frac{4\pi^2}{3\hbar} \frac{l}{\lambda} \rho |A|^2 h(u, v) d_e \mathcal{E} \frac{R_d[i, J|M_J|] + R_d[f, J'|M_{J'}|]}{\Gamma_D^2}. \tag{20}$$

The absorption cross-section for the resonance case for the light propagating through a medium can be presented as

$$\sigma(u) = \sigma_0 f(u, v) = \frac{4\pi}{3\hbar c} \frac{\omega_0}{\Gamma_D} f(u, v) |A_{\text{total}}|^2, \tag{21}$$

where σ_0 is the absorption cross-section at the point of resonance and A_{total} is the total amplitude that includes the contribution of the considered transition process and possible other decay channels if exist. However in the cases of the resonant absorption which will be discussed in the next section we can neglect other decay channels and assume that $|A_{\text{total}}| = A$. The comment can be made on the behavior of the spectral line shape for the considered $\mathcal{P}, \mathcal{T}$-odd Faraday effect. The function $g(u, v)$ describes the behavior of the optical rotation angle in the case of natural or $\mathcal{P}$-odd optical activity in the vicinity of the resonance. In case of the $\mathcal{P}$-odd optical rotation the difference in refractive indices for the left- and the right-circularly polarized light is defined by $\text{Re}(n^+ - n^-) = 4\mathcal{P}(\text{Re} n(\omega) - 1)$ (see Equation (1)) where $\mathcal{P}$ is referred to as the degree of circular polarization of the light or the degree of parity nonconservation. Then, according to Equations (2) and (3), the line shape is antisymmetric with respect to the resonance frequency ω_0. The function $f(u, v)$ describes the absorption line profile in the vicinity of the resonance. For more details the reader is referred to the book [41]. The function $h(u, v)$ describes the rotation angle caused by the $\mathcal{P}, \mathcal{T}$-odd Faraday effect close to the resonance frequency. This function has two maxima (by absolute value): one maximum corresponds to the point of the resonance coinciding with the maximum of absorption and another maximum is off the resonance

where absorption is small. This second maximum should allow working off-resonance when searching for the $\mathcal{P},\mathcal{T}$-odd Faraday effect with the large optical path length.

If the nuclear spin is not equal to zero there is another mechanism which can affect the refractive index. The electric field with consideration of the $\mathcal{P},\mathcal{T}$-odd effects leads to the mixing of the states with different hyperfine levels F but the same projection M_F. As a result there appears the contribution proportional to the line profile $g(u,v)$ for the $\mathcal{P},\mathcal{T}$-odd Faraday effect (the derivation of this result is completely analogous to the ordinary Faraday effect consideration in [47]). However this contribution is suppressed by several orders of magnitude by the factor of $\Delta\omega/\Delta_{\mathrm{hfs}} \sim \Gamma_D/\Delta_{\mathrm{hfs}}$ (where Δ_{hfs} is the hyperfine splitting) and thus can be neglected.

Introduce now the product of the $\mathcal{P},\mathcal{T}$-odd Faraday rotation angle $\psi(u)$ and the transmitted light intensity function $T(u)$ which is referred to as the signal $R(u)$:

$$R(u) = \psi(u)T(u). \tag{22}$$

The transmission function $T(u)$ is governed by the Beer-Lambert-Bouguer law

$$T(u) = e^{-lL^{-1}(u)}, \tag{23}$$

where $L(u)$ is the absorption length at the point of detuning u.

$$L^{-1}(u) = \rho\sigma(u) = \rho\sigma_0 f(u,v) = \frac{4\pi}{3\hbar c}\rho\frac{\omega_0}{\Gamma_D}f(u,v)|A|^2. \tag{24}$$

It is widely known that the shot-noise limit is proportional to the square root of the number of detected photons. So the signal-to-noise ratio and statistical sensitivity $(R(u)/\sqrt{T(u)})$ is optimal when $\frac{d}{dl}\left(le^{-l/2L(u)}\right) = 0$, i.e., when $l = 2L(u)$. From this condition the expression for the optimal column density ρl reads

$$\rho l = \frac{3\hbar c}{2\pi}\frac{\Gamma_D}{f(u,v)\omega_0|A|^2}. \tag{25}$$

It is more convenient to rewrite Equation (24) in terms of the natural width of the excited state Γ_n:

$$\rho l = \frac{2\omega_0^2}{\pi c^2}\frac{\Gamma_D}{f(u,v)\Gamma_n}. \tag{26}$$

Please note that in the case of M1 transition when the collisional broadening effects should be considered and $v = v(\rho)$, Equations (24) and (25) define $\rho = \rho(l)$. Substituting ρl from Equation (24) to Equation (20) one gets the expression for the maximum rotation angle

$$\psi_{\mathrm{max}}(u) = \frac{h(u,v)}{f(u,v)}\frac{d_e\mathcal{E}\left(R_d^i + R_d^f\right)}{\Gamma_D}. \tag{27}$$

Let us analyse the expression (27). Since for the $\mathcal{P},\mathcal{T}$-odd Faraday effect we are interested in the off-resonance measurement when the second maximum is achieved, then we can use known asymptotics for functions h and f: $h(u,v) \sim 1/u^2$ and $f(u,v) \sim v/u^2$. As it will be shown in the next section this asymptotics is valid already for $u = 4$ where the rotation angle achieves its maximum. Then

$$\psi_{\mathrm{max}}(u) = \frac{2}{\Gamma}d_e\mathcal{E}\left(R_d^i + R_d^f\right). \tag{28}$$

From Equation (27) it follows that for E1 transitions this maximum value cannot be further increased with increasing of the column density or reducing the Doppler width (cooling of atomic vapor). It is also obvious that for transitions of M1 type the effect can be increased with diminishing the value of ρ together with increasing the optical path length l while collisional

broadening dominates over the natural width of the transition line (see Section 3). In case of resolving the hyperfine transitions then the hyperfine structure factors about (0.1–1.0) appear for the R_d coefficients (for E1 and M1) as well as for the natural line width (only for E1) of the excited state in Equation (27). It is obvious that taking account for the hyperfine structure does not change the estimate of the rotation angle for the $\mathcal{P},\mathcal{T}$-odd Faraday effect.

3. Application to Transitions in Different Atomic Species

3.1. Ra Atom (Z = 88)

Let us consider the transition $6p^2 7s^2{}^1S_0 \to 6p^2 7s7p^3P_1$ of E1 type for the radium atom with the transition wavelength $\lambda = 714$ nm. For our estimates of the rotation angle we take the value for the eEDM enhancement factor of the final (excited) state from [18]: $\left(R_d^i + R_d^f\right) = (0 + (-1955)) = -1955$. In what follows the estimates for the $\mathcal{P},\mathcal{T}$-odd Faraday rotation angle are made for the electron EDM effect at the level of $d_e \approx 10^{-29}$ e cm (the bound established in the experiment with the ThO molecule [13]). For an external electric field we set the maximum achievable in laboratory value $\mathcal{E} = 10^5$ V/cm [10]. Assuming the room temperature $T \sim 300$ K and employing the transition frequency value $\omega_0 = 2.7 \times 10^{15}$ s^{-1}, according to Equation (19) we obtain the Doppler width $\Gamma_D \approx 1.3 \times 10^9$ s^{-1}. The natural line width for the chosen transition is $\Gamma_n = 2.37 \times 10^6$ s^{-1} [48]. Our estimation of the maximum $\mathcal{P},\mathcal{T}$-odd Faraday angle and the corresponding column density according to Equation (27) and Equation (26) depicted in Figure 2a,b, respectively.
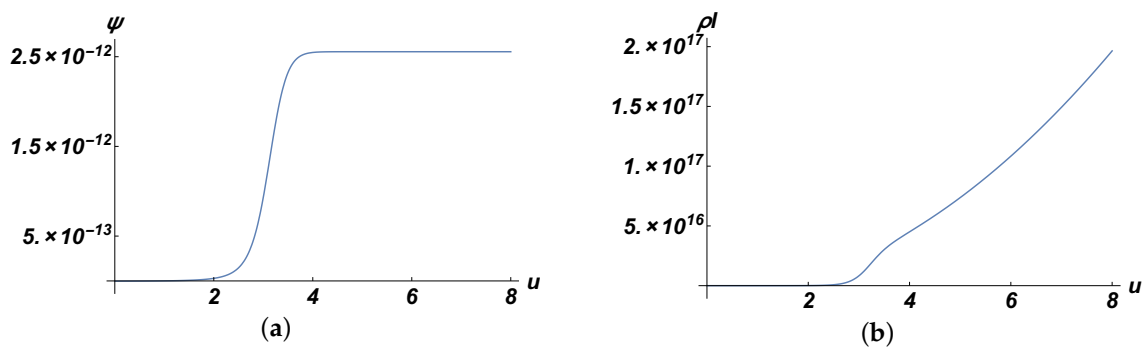

Figure 2. (**a**) represents the behavior of the maximum value of the $\mathcal{P},\mathcal{T}$-odd Faraday angle ψ (in rad) on the dimensionless detuning u for the E1 transition $6p^2 7s^2{}^1S_0 \to 6p^2 7s7p^3P_1$ in Ra atom, (**b**) represents the behavior of the column density ρl (in cm^{-2}) on the dimensionless detuning u for the E1 transition $6p^2 7s^2{}^1S_0 \to 6p^2 7s7p^3P_1$ in Ra atom.

From Figure 2a it follows that maximum rotation angle is achieved already at the detuning $u = 4$. As this takes place,

$$\psi_{\max}(u = 4) \approx 2.6 \times 10^{-12} \text{ rad} \tag{29}$$

for the observation of the electron EDM of the order $d_e = 10^{-29}$ e cm. The column density that is needed for this $\rho l \approx 5 \times 10^{16}$ cm^{-2}. Such column density can be easily obtained in the cavity of 1 m long and optical path length equal to 100 km described in [38]. However, in fact, the electric field $\mathcal{E} = 10^5$ V/cm can be easily produced only within a small volume of the size 1 cm. As a result, the optical path length is scaled down to 1 km. Nevertheless, assuming $l = 1$ km we obtain the optimal density $\rho_{\text{opt}} \approx 5 \times 10^{11}$ cm^{-3} that in principle can be prepared. Note also that through the use of asymptotics of $h(u, v)$ and $f(u, v)$ we arrive at the same result as in Equation (29). Then in what follows we will employ the asymptotics and use for the estimation of the $\mathcal{P},\mathcal{T}$-odd Faraday angle Equation (28). The best sensitivity was reported in [40] where the birefringence phase shift of the order 3×10^{-13} rad was registered. If one assumes this record sensitivity, then the Ra atom appears to be a good candidate for improving the eEDM bound by an order of magnitude.

3.2. Pb Atom (Z = 82)

In the case of the lead atom we consider two transitions: of E1 type and of M1 type.

(1) The first one is the E1 $6p^2(1/2, 1/2)_0 \rightarrow 6p7s(1/2, 1/2)_1$ with the transition wavelength $\lambda = 283$ nm. We employ the value for the eEDM enhancement factor of the $6p7s(1/2, 1/2)_1$ state from [18]: $\left(R_d^i + R_d^f \right) = (0 + (844)) = 844$. Assuming $T \sim 300$ K and employing $\omega_0 = 6.7 \times 10^{15}$ s^{-1}, according to Equation (19) $\Gamma_D \approx 3.4 \times 10^9$ s^{-1}. The natural line width for the chosen transition is $\Gamma_n = 1.79 \times 10^8$ s^{-1} [49]. For $\mathcal{E} = 10^5$ V/cm, $d_e = 10^{-29}$ e cm and $u \approx 4$ from Equation (28) it follows

$$\psi_{\text{max}} \approx 1.6 \times 10^{-14} \text{ rad.} \tag{30}$$

The necessary column density appears to be $\rho l \approx 3.7 \times 10^{14}$ cm^{-2}. This result shows that the best possible estimate for the eEDM with the maximum modern sensitivity achievement ($\sim 10^{-13}$ rad [40]) would be still an order of magnitude above the value quoted in [13].

(2) Now we consider the M1 transition $6p^2(1/2, 1/2)_0 \rightarrow 6p^2(3/2, 1/2)_1$ with $\lambda = 1279$ nm. Here we also employ the value for the eEDM enhancement factor of the $6p^2(3/2, 1/2)_1$ state from [18]: $\left(R_d^i + R_d^f \right) = (0 + 234) = 234$. Assuming $T \sim 300$ K and employing $\omega_0 = 1.5 \times 10^{15}$ s^{-1}, according to Equation (19) $\Gamma_D \approx 7.7 \times 10^8$ s^{-1}. The natural line width for the chosen transition (for the $6p^2(3/2, 1/2)_1$ metastable state) is $\Gamma_n = 7$ s^{-1} according to [49]. Let us estimate the value of the collisional broadening Γ_{col} according to Equation (4). The characteristic value for the collisional cross-section is $\sigma_{\text{col}} \approx 0.5 \times 10^{-14}$ cm^2 [41]. Then in terms of density ρ we obtain $\Gamma_{\text{col}} = 7.6 \times 10^{-11} \rho[\text{cm}^{-3}]$ s^{-1}. So in this case the dimensionless $v = \frac{\Gamma}{2\Gamma_D} \approx 4.6 \times 10^{-9} + 10^{-19} \rho[\text{cm}^{-3}]$. It appears that for $\rho > 10^{11}$ cm^{-3} the collisional broadening mechanism dominates over the natural broadening one. Since now the maximum rotation angle (Equation (28)) (optimal for the experiment) depends on ρ ($\psi_{\text{max}} \sim 1/\rho$) and the column density according to Equation (26) is not fixed (the fixed quantity is $\rho^2 l$, i.e., $1/\rho \sim \sqrt{l}$) then let us employ the maximum feasible value for the optical path lengths in our estimates. In [39] path length of 70,000 km for the cavity of the same size as in [38] was reported. If such a large electric field ($\mathcal{E} = 10^5$ V/cm) can be implemented in the cavity in a volume of a several centimetres size then the optical path length appears to be $l = 10^8$ cm. It corresponds to the optimal number density, according to Equation (26), $\rho \approx 5 \times 10^{14}$ cm^{-3}. Then, for $d_e = 10^{-29}$ e cm and $u \approx 4$ from Equation (28) it follows

$$\psi_{\text{max}} \approx 1.1 \times 10^{-11} \text{ rad.} \tag{31}$$

Thus, if to assume the record sensitivity [40] and the record optical path length [39], then the lead atom appears to be a good candidate for improving the eEDM bound by 2 orders of magnitude.

3.3. Tl Atom (Z = 81)

For the thallium atom we consider the $6p_{1/2} \rightarrow 6p_{3/2}$ transition of M1 type with $\lambda = 1283$ nm. We employ the values for the eEDM enhancement factor of the ground and excited metastable state from [18]: $\left(R_d^i + R_d^f \right) = (-526 + 7) = -519$. Assuming $T \sim 300$ K and employing $\omega_0 = 1.5 \times 10^{15}$ s^{-1}, according to Equation (19) $\Gamma_D \approx 7.7 \times 10^8$ s^{-1}. The natural line width for the chosen transition (for the $6p_{3/2}$ metastable state) is $\Gamma_n = 4$ s^{-1} according to [49]. Similar to the case of M1 transition in Pb, in terms of density ρ we obtain $\Gamma_{\text{col}} = 7.6 \times 10^{-11} \rho[\text{cm}^{-3}]$ s^{-1}. So the dimensionless $v = \frac{\Gamma}{2\Gamma_D} \approx 2.6 \times 10^{-9} + 10^{-19} \rho[\text{cm}^{-3}]$. For $l = 10^8$ cm the corresponding number density according to Equation (26) $\rho \approx 6.6 \times 10^{14}$ cm^{-3}. Then, for $d_e = 10^{-29}$ e cm, $\mathcal{E} = 10^5$ V/cm and $u \approx 4$ from Equation (28) it follows

$$\psi_{\text{max}} \approx 2 \times 10^{-11} \text{ rad.} \tag{32}$$

Thus, assuming the record sensitivity [40] and the record optical path length [39], the thallium atom appears to be a good candidate for improving the *e*EDM bound by 2 orders of magnitude.

3.4. Hg Atom (Z = 80)

In the case of the mercury atom we consider two E1 transitions:

(1) The first one is from the metastable $6s6p(^3P_1)$ state to the excited $6s7s(^3S_1)$ state with $\lambda = 436$ nm. The population of the lower metastable level can be obtained with the laser pumping [38]. The *e*EDM enhancement factors were calculated in [42] and $\left(R_d^i + R_d^f\right) = (-427 + 893) = 466$. In [42] R_d factors are presented for definite hyperfine levels. Here these values are recalculated for the levels $i, J|M_J|$ and $f, J'|M_{J'}|$. The natural line width for the chosen transition is $\Gamma_n = 1.0 \times 10^8$ s^{-1} [49]. Assuming the room temperature $T \sim 300$ K and employing the transition frequency value $\omega_0 = 4 \times 10^{15}$ s^{-1}, according to Equation (19) we obtain the value for the Doppler width $\Gamma_D = 5.2 \times 10^{-7}\omega_0 \approx 2 \times 10^9$ s^{-1}. For $\mathcal{E} = 10^5$ V/cm, $d_e = 10^{-29}$ *e* cm and $u \approx 4$ from Equation (28) it follows

$$\psi_{\max} \approx 8 \times 10^{-15} \text{ rad}. \tag{33}$$

The necessary column density appears to be $\rho l \approx 1.5 \times 10^{14}$ cm^{-2}. This result shows that the best possible estimate for the *e*EDM with the maximum modern sensitivity achievement ($\sim 10^{-13}$ rad [40]) would be still 2 orders of magnitude above the value quoted in [13].

(2) The second transition of E1 type is from the ground $6s^2(^1S_0)$ to the metastable $6s6p(^3P_1)$ state with $\lambda = 254$ nm. According to [42], $\left(R_d^i + R_d^f\right) = (0 + (-427)) = 427$. Employing $\omega_0 = 7.4 \times 10^{15}$ s^{-1}, according to Equation (19), $\Gamma_D = 5.2 \times 10^{-7}\omega_0 \approx 3.7 \times 10^9$ s^{-1}. The natural line width for the chosen transition is $\Gamma_n = 2.0 \times 10^7$ s^{-1}. For $\mathcal{E} = 10^5$ V/cm, $d_e = 10^{-29}$ *e* cm and $u \approx 4$ from Equation (28) it follows

$$\psi_{\max} \approx 8 \times 10^{-14} \text{ rad}. \tag{34}$$

The necessary column density appears to be $\rho l \approx 4.2 \times 10^{16}$ cm^{-2}. This result shows that the best possible estimate for the *e*EDM with the maximum modern sensitivity achievement ($\sim 10^{-13}$ rad [40]) could give the same upper bound for *e*EDM as already quoted in [13].

3.5. Cs Atom (Z = 55)

For the caesium atom we consider the transition $6s_{1/2} \rightarrow 6p_{1/2}$ with $\lambda = 895$ nm. Let us employ the value for the *e*EDM enhancement factors of the ground and excited states from [18]: $\left(R_d^i + R_d^f\right) = (107 + (-194)) = -87$. Assuming $T \sim 300$ K and employing $\omega_0 = 2.1 \times 10^{15}$ s^{-1}, according to Equation (19) $\Gamma_D \approx 1.4 \times 10^9$ s^{-1}. The natural line width for the chosen transition is $\Gamma_n = 3.23 \times 10^7$ s^{-1} [49]. For $\mathcal{E} = 10^5$ V/cm, $d_e = 10^{-29}$ *e* cm and $u \approx 4$ from Equation (28) it follows

$$\psi_{\max} \approx 9.2 \times 10^{-14} \text{ rad}. \tag{35}$$

The necessary column density appears to be $\rho l \approx 1.9 \times 10^{14}$ cm^{-2}. This result shows that the best possible estimate for the *e*EDM with the maximum modern sensitivity achievement ($\sim 10^{-13}$ rad [40]) could give the same upper bound for *e*EDM as already quoted in [13].

3.6. Xe Atom (Z = 54)

The last considered example is the E1 transition from the metastable $(^2P_{3/2}^0)6s[3/2]_2^0$ state to the excited $(^2P_{3/2}^0)6p[1/2]_1$ state of the xenon atom with $\lambda = 980$ nm The population of the lower metastable level can be obtained with the laser pumping [38]. The *e*EDM enhancement factors

were calculated in [42] and $\left(R_d^i + R_d^f\right) = (113 + (-48)) = 65$. In [42] R_d factors are presented for definite hyperfine levels. Here these values are recalculated for the levels $i, J|M_J|$ and $f, J'|M_{J'}|$. Assuming the room temperature $T \sim 300$ K and employing the transition frequency value $\omega_0 = 2 \times 10^{15}$ s^{-1}, according to Equation (19) we obtain the Doppler width $\Gamma_D = 6.5 \times 10^{-7}\omega_0 \approx 1.3 \times 10^9$ s^{-1}. The natural line width for the chosen transition is $\Gamma_n = 2.6 \times 10^7$ s^{-1} [49]. For $\mathcal{E} = 10^5$ V/cm, $d_e = 10^{-29}$ e cm and $u \approx 4$ from Equation (28) it follows

$$\psi_{\max} \approx 9 \times 10^{-15} \text{ rad.} \tag{36}$$

The necessary column density appears to be $\rho l \approx 2.2 \times 10^{14}$ cm^{-2}. This result shows that the best possible estimate for the eEDM with the maximum modern sensitivity achievement ($\sim 10^{-13}$ rad [40]) would be still an order of magnitude above the value quoted in [13].

The summary of the results of this section is presented in Table 1.

Table 1. The summary of the results of the $\mathcal{P},\mathcal{T}$-odd Faraday optical rotation theoretical simulation for different atomic species. The maximum $\mathcal{P},\mathcal{T}$-odd Faraday rotation angle $\psi_{\max}$ (in rad) corresponds to an external electric field $\mathcal{E} = 10^5$ V/cm [10] and to the present eEDM bound established in experiments with ThO molecules ($d_e = 10^{-29}$ e cm [13]).

Atom	Transition	Wavelength λ, nm	Linewidth Γ_n, s^{-1}	Column Density ρl, cm^{-2}	Rotation Angle $\psi_{\max}$, rad
Ra	$6p^2 7s^2\,{}^1S_0 \rightarrow 6p^2 7s 7p\,{}^3P_1$ (M1)	714	2.37×10^6	5.0×10^{16}	2.6×10^{-12}
Pb	$6p^2(1/2,1/2)_0 \rightarrow 6p7s(1/2,1/2)_1$ (E1)	283	1.79×10^8	3.7×10^{14}	1.6×10^{-14}
Pb	$6p^2(1/2,1/2)_0 \rightarrow 6p^2(3/2,1/2)_1$ (M1)	1279	7	5.0×10^{22}	1.1×10^{-11}
Tl	$6p_{1/2} \rightarrow 6p_{3/2}$ (M1)	1283	4	6.6×10^{22}	2.0×10^{-11}
Hg	$6s6p(^3P_1) \rightarrow 6s7s(^3S_1)$ (E1)	436	1.0×10^8	1.5×10^{14}	8.0×10^{-15}
Hg	$6s^2(^1S_0) \rightarrow 6s6p(^3P_1)$ (E1)	254	2.0×10^7	4.2×10^{16}	8.0×10^{-14}
Cs	$6s_{1/2} \rightarrow 6p_{1/2}$ (E1)	895	3.23×10^7	1.9×10^{14}	9.2×10^{-14}
Xe	$(^2P^0_{3/2})6s[3/2]^0_2 \rightarrow (^2P^0_{3/2})6p[1/2]_1$ (E1)	980	2.6×10^7	2.2×10^{14}	9.0×10^{-15}

4. Conclusion

The main result of the study reported in this paper is that the M1 transitions in the Tl and Pb atoms as well as the E1 transitions in the Ra, Hg and Cs atoms are favorable for the observation of the $\mathcal{P},\mathcal{T}$-odd Faraday optical rotation for the cavity-enhanced technique and ICAS experiments discussed in [38–40]. For the M1 transitions a very large optical path length (of about 10^3 km) is required. To sum up, optimistically under abovementioned experimental conditions the eEDM border can be shifted down by one or two orders of magnitude compared to the recent experimental bound. Please note that in such optical experiments the $\mathcal{P}$-odd optical rotation also occurs which is, in fact, vastly larger than the $\mathcal{P},\mathcal{T}$-odd Faraday optical rotation. However, the ordinary optical activity (including the $\mathcal{P}$-odd effects) effect cancels after the light travels onward and backward in the cavity. The $\mathcal{P},\mathcal{T}$-odd and ordinary Faraday activity effect grows up after such round-trip.

Let us give a brief comment also on the systematic errors in this optical rotation experiment. It is easily seen that the motional magnetic field which appears in the atomic frame due to the chaotic motion of atoms in the cavity cannot mimic the electron EDM effect since it is always orthogonal to the applied electric field. The possible avoiding of the uncontrolled external static magnetic fields influence can be achieved if simultaneously with the observation of the $\mathcal{P},\mathcal{T}$-odd Faraday optical rotation, the ordinary Faraday optical rotation in the applied external magnetic field parallel to the applied external electric field will be measured. Then switching of the electric field direction cancels the influence of the uncontrolled magnetic fields. In this case, only uncontrolled alternating magnetic fields with a frequency close to the inverse time of the electric field switching can be dangerous. A general problem of excluding the electromagnetic field fluctuations can be in principle addressed by the use of more intensive lasers (see [18]).

Directions for future research may be the usage of molecule beams passing through such a cavity for the search of the eEDM by means of the $\mathcal{P},\mathcal{T}$-odd Faraday optical rotation. Molecules usually possess much larger enhancement coefficients of the eEDM than heavy atoms.

References

1. Pospelov, M.; Khriplovich, I. Electric dipole moment of the W boson and the electron in the Kobayashi-Maskawa model. *Sov. Nucl. Phys.* **1991**, *53*, 638.
2. Salpeter, E.E. Some atomic effects of an electronic electric dipole moment. *Phys. Rev.* **1958**, *112*, 1642. [CrossRef]
3. Sandars, P.G.H. The electric dipole moment of an atom. *Phys. Lett.* **1965**, *14*, 194. [CrossRef]
4. Sandars, P.G.H. The search for violation of P or T invariance in atoms or molecules. *At. Phys.* **1975**, *4*, 71.
5. Gorshkov, V.G.; Labzowsky, L.N.; Moskalev, A.N. Space and time parity nonconservation effects in the diatomic molecule spectra. *Sov. Phys. JETP* **1979**, *49*, 209.
6. Pospelov, M.; Ritz, A. CKM benchmarks for electron electric dipole moment experiments. *Phys. Rev. D* **2014**, *89*, 056006. [CrossRef]
7. Chubukov, D.V.; Labzowsky, L.N. P, T-odd electron-nucleus interaction in atomic systems as an exchange by Higgs bosons. *Phys. Rev. A* **2016**, *93*, 062503. [CrossRef]
8. Bondarevskaya, A.A.; Chubukov, D.V.; Andreev, O.Y.; Mistonova, E.A.; Labzowsky, L.N.; Plunien, G.; Liesen, D.; Bosch, F. On the electric dipole moment of the electron and the P, T-odd electron-nucleus interaction in highly-charged heavy ions. *J. Phys. B* **2015**, *48*, 144007. [CrossRef]
9. Ginges, J.S.; Flambaum, V.V. Violations of fundamental symmetries in atoms and tests of unification theories of elementary particles. *Phys. Rep.* **2004**, *397*, 63–154. [CrossRef]
10. Regan, B.C.; Commins, E.D.; Schmidt, C.J.; DeMille, D. New limit on the electron electric dipole moment. *Phys. Rev. Lett.* **2002**, *88*, 071805. [CrossRef]
11. Hudson, J.J.; Kara, D.M.; Smallman, I.J.; Sauer, B.E. Tarbutt, M.R.; Hinds, E.A.; Improved measurement of the shape of the electron. *Nature* **2011**, *473*, 493. [CrossRef] [PubMed]
12. Baron, J.; Campbell, W.C.; DeMille, D.; Doyle, J.M.; Gabrielse, G.; Gurevich, Y.V.; Hess, P.W.; Hutzler, N.R.; Kirilov, E.; Kozyryev, I.; et al. Order of magnitude smaller limit on the electric dipole moment of the electron. *Science* **2014**, *343*, 269–272.
13. Andreev, V.; Hutzler, N.R. Improved limit on the electric dipole moment of the electron. *Nature* **2018**, *562*, 355–360.
14. Cairncross, W.B.; Gresh, D.N.; Grau, M.; Cossel, K.C.; Roussy, T.S.; Ni, Y.; Zhou, Y.; Ye, J.; Cornell, E.A. Precision measurement of the electron's electric dipole moment using trapped molecular ions. *Phys. Rev. Lett.* **2017**, *119*, 153001. [CrossRef]
15. Liu, Z.W.; Kelly, H.P. Analysis of atomic electric dipole moment in thallium by all-order calculations in many-body perturbation theory. *Phys. Rev. A* **1992**, *45*, R4210(R). [CrossRef]
16. Dzuba, V.A.; Flambaum, V.V. Calculation of the (T,P)-odd electric dipole moment of thallium and cesium. *Phys. Rev. A* **2009**, *80*, 062509. [CrossRef]
17. Porsev, S.G.; Safronova, M.S.; Kozlov, M.G. Electric dipole moment enhancement factor of thallium. *Phys. Rev. Lett.* **2012**, *108*, 173001. [CrossRef]
18. Chubukov, D.V.; Skripnikov, L.V.; Labzowsky, L.N. P,T-odd Faraday rotation in heavy neutral atoms. *Phys. Rev. A* **2018**, *97*, 062512. [CrossRef]
19. Quiney, H.M.; Skaane, H.; Grant, I.P. Hyperfine and PT-odd effects in YbF. *J. Phys. B* **1998**, *31*, 85. [CrossRef]
20. Parpia, F. Ab initio calculation of the enhancement of the electric dipole moment of an electron in the YbF molecule. *J. Phys. B* **1998**, *31*, 1409. [CrossRef]

21. Mosyagin, N.S.; Kozlov, M.G.; Titov, A.V. Electric dipole moment of the electron in the YbF molecule. *J. Phys. B At. Mol. Opt. Phys.* **1998**, *31*, L763. [CrossRef]

22. Abe, M.; Gopakumar, G.; Hada, M.; Das, B.P.; Tatewaki, H.; Mukherjee, D. Application of relativistic coupled-cluster theory to the effective electric field in YbF. *Phys. Rev. A* **2014**, *90*, 022501. [CrossRef]

23. Skripnikov, L.V.; Petrov, A.N.; Titov, A.V. Communication: Theoretical study of ThO for the electron electric dipole moment search. *J. Chem. Phys.* **2013** *139*, 221103. [CrossRef]

24. Skripnikov, L.V.; Titov, A.V. Theoretical study of thorium monoxide for the electron electric dipole moment search: Electronic properties of $H^3\Delta 1$ in ThO. *J. Chem. Phys.* **2015**, *142*, 024301. [CrossRef] [PubMed]

25. Skripnikov, L.V. Combined 4-component and relativistic pseudopotential study of ThO for the electron electric dipole moment search. *J. Chem. Phys.* **2016**, *145*, 214301. [CrossRef] [PubMed]

26. Denis, M.; Fleig, T. In search of discrete symmetry violations beyond the standard model: Thorium monoxide reloaded. *J. Chem. Phys.* **2016**, *145*, 214307. [CrossRef] [PubMed]

27. Petrov, A.N.; Mosyagin, N.S.; Isaev, T.A.; Titov, A.V. Theoretical study of HfF^+ in search of the electron electric dipole moment. *Phys. Rev. A* **2007**, *76*, 030501(R). [CrossRef]

28. Skripnikov, L.V. Communication: Theoretical study of HfF^+ cation to search for the T,P-odd interactions. *J. Chem. Phys.* **2017**, *147*, 021101. [CrossRef] [PubMed]

29. Fleig, T. P,T-odd and magnetic hyperfine-interaction constants and excited-state lifetime for HfF^+. *Phys. Rev. A* **2017**, *96*, 040502 . [CrossRef]

30. Petrov, A.N.; Skripnikov, L.V.; Titov, A.V.; Flambaum, V.V. Evaluation of C P violation in HfF^+. *Phys. Rev. A* **2018**, *98*, 042502. [CrossRef]

31. Zel'dovich, Y.B. Parity nonconservation in the first Order in the weak-interaction constant in electron scattering and other Effects. *Sov. Phys. JETP* **1959**, *9*, 682.

32. Khriplovich, I.B. Feasibility of observing parity nonconservation in atomic transitions. *Sov. Phys. JETP Letters* **1974**, *20*, 315.

33. Barkov, L.M.; Zolotorev, M.S. Observation of parity non-conservation in atomic transitions. *Sov. Phys.* **1978**, *27*, 357.

34. Baranova, N.B.; Bogdanov, Y.V.; Zel'dovich, B.Y. New electro-optical and magneto-optical effects in liquids. *Sov.Phys.Usp* **1977**, *20*, 870. [CrossRef]

35. Sushkov, O.P.; Flambaum, V.V. Parity breaking effects in diatomic molecules. *Sov. Phys. JETP* **1978**, *48*, 608.

36. Budker, D.; Gawlik, W.; Kimball, D.; Rochester, S.M.; Yashchuk,V.; Weis, A. Resonant nonlinear magneto-optical effects in atoms. *Rev. Mod. Phys.* **2002**, *74*, 1153. [CrossRef]

37. Chubukov, D.V.; Labzowsky, L.N. P,T-odd Faraday effect in intracavity absorption spectroscopy. *Phys. Rev. A* **2017**, *96*, 052105. [CrossRef]

38. Bougas, L.; Katsoprinakis, G.E.; von Klitzing, W.; Rakitzis, T.P. Fundamentals of cavity-enhanced polarimetry for parity-nonconserving optical rotation measurements: Application to Xe, Hg, and I. *Phys. Rev. A* **2014**, *89*, 052127. [CrossRef]

39. Baev, V.M.; Latz, T.; Toschek, P.E. Laser intracavity absorption spectroscopy. *Appl. Phys. B* **1999**, *69*, 171–202. [CrossRef]

40. Durand, M.; Morville, J.; Romanini, D. Shot-noise-limited measurement of sub-parts-per-trillion birefringence phase shift in a high-finesse cavity. *Phys. Rev. A* **2010**, *82*, 031803. [CrossRef]

41. Khriplovich, I.B. *Parity Nonconservation in Atomic Phenomena*; Gordon and Breach: London, UK, 1991.

42. Chubukov, D.V.; Skripnikov, L.V.; Labzowsky, L.N.; Kutuzov, V.N.; Chekhovskoi, S.D. Evaluation of the P,T-odd Faraday effect in Xe and Hg atoms. *Phys. Rev. A* **2019**, *99*, 052515. [CrossRef]

43. Johnson, W.R.; Guo, D.S.; Idrees, M.; Sapirstein, J. Weak-interaction effects in heavy atomic systems. II. *Phys.Rev. A* **1986**, *34*, 1043. [CrossRef]

44. Lindroth, E.; Lynn, B.W.; Sandars, P.G.H. Order $\alpha 2$ theory of the atomic electric dipole moment due to an electric dipole moment on the electron. *J. Phys. B* **1989**, *22*, 559. [CrossRef]

45. Skripnikov, L.V.; Titov, A.V.; Petrov, A.N.; Mosyagin, N.S.; Sushkov, O.P. Enhancement of the electron electric dipole moment in Eu^{2+} *Phys. Rev. A* **2011**, *84*, 022505. [CrossRef]

46. Skripnikov, L.V.; Maison, D.E.; Mosyagin, N.S. Scalar-pseudoscalar interaction in the francium atom. *Phys. Rev. A* **2017**, *95*, 022507. [CrossRef]

47. Roberts, G.J.; Baird, P.E.G.; Brimicombe, M.W.S.M.; Sandars, P.G.H.; Selby, D.R.; Stacey, D.N. The Faraday effect and magnetic circular dichroism in atomic bismuth. *J. Phys. B At. Mol. Phys.* **1980**, *13*, 1389. [CrossRef]

48. Scielzo, N.D.; Guest, J.R.; Schulte, E.C.; Ahmad, I.; Bailey, K.; Bowers, D.L.; Holt, R.J.; Lu, Z.-T.; O'Connor, T.P.; Potterveld, D.H. Measurement of the lifetimes of the lowest 3P1 state of neutral Ba and Ra. *Phys. Rev. A* **2006**, *73*, 010501(R). [CrossRef]

49. Radzig, A.A.; Smirnov, B.M. *Reference Data on Atoms, Molecules, and Ions*; Springer: Berlin, Germany, 1985.